MATHEMATICAL BIOSCIENCES
AND ENGINEERING
Volume **13**, Number **3**, June **2016**

doi:10.3934/mbe.2016005

pp. **521–535**

INTEGRATOR OR COINCIDENCE DETECTOR — WHAT SHAPES THE RELATION OF STIMULUS SYNCHRONY AND THE OPERATIONAL MODE OF A NEURON?

Achilleas Koutsou

Department of Computer Science, University of Cyprus
1678 Nicosia, Cyprus

Jacob Kanev

Department of Electrical Engineering and Computer Science
Technische Universität Berlin, 10587 Berlin, Germany

Maria Economidou and Chris Christodoulou

Department of Computer Science, University of Cyprus
1678 Nicosia, Cyprus

Abstract. The operational mode of a neuron (i.e., whether a neuron is an integrator or a coincidence detector) is in part determined by the degree of synchrony in the firing of its pre-synaptic neural population. More specifically, it is determined by the degree of synchrony that causes the neuron to fire. In this paper, we investigate the relationship between the input and the operational mode. We compare the response-relevant input synchrony, which measures the operational mode and can be determined using a membrane potential slope-based measure [7], with the spike time distance of the spike trains driving the neuron, which measures spike train synchrony and can be determined using the multivariate SPIKE-distance metric [10]. We discover that the relationship between the two measures changes substantially based on the values of the parameters of the input (firing rate and number of spike trains) and the parameters of the post-synaptic neuron (synaptic weight, membrane leak time constant and spike threshold). More importantly, we determine how the parameters interact to shape the synchrony-operational mode relationship. Our results indicate that the amount of depolarisation caused by a highly synchronous volley of input spikes, is the most influential factor in defining the relationship between input synchrony and operational mode. This is defined by the number of input spikes and the membrane potential depolarisation caused per spike, compared to the spike threshold.

1. **Introduction.** The mechanisms used by neurons to encode information into spike trains is one of the fundamental questions surrounding the neural code. In 1982, Abeles proposed that neurons in the cortex may act as coincidence detectors rather than temporal integrators [1]. *Temporal integration* implies that neurons fire a response after a certain number of pre-synaptic spikes (on average) arrive at the neuron's input [16, 17]. Under this assumption, the temporal structure of pre-synaptic spike trains is lost in the integration process of the post-synaptic neuron. The firing rate of the post-synaptic neuron encodes the intensity (i.e., the rate) of

2010 *Mathematics Subject Classification.* 92B25, 92C20, 92-08.

Key words and phrases. Operational mode, membrane potential slope, input synchrony, spike distance metrics, coincidence detection, temporal integration.

the total (summed) pre-synaptic activity. On the other hand *coincidence detection* implies that the firing of a neuron is a result of synchronous arrival of multiple input spikes and that temporally dispersed spike trains are unable (or less likely) to cause a neuron to fire [18, 19].

While it is relatively straightforward to show that a passive model neuron can be excited by both temporally dispersed and precisely coincident activity [5, 2, 14], the existence of the latter has great implications for the nature of the neural code [18, 19, 6, 3]. In particular, if coincidence detection was indeed found to be the dominant mode of operation in certain neurons, it would indicate an increased significance of precise timing in spike trains, which greatly reinforces and supports the existence of temporal codes, as opposed to rate codes [18, 19, 6].

We recently described a measure that estimates the degree of response-relevant synchrony between the set of pre-synaptic spike trains driving a leaky integrate-and-fire (LIF) neuron, obtained by observing the intracellular potential slope prior to depolarisation and assuming no knowledge of the actual pre-synaptic firing activity [7]. Our measure however, referred to here as the Normalised Pre-Spike Slope (NPSS), is more than just an input synchrony estimator. Given that it measures the response-relevant input synchrony, i.e., the degree of synchrony that is responsible for triggering response spikes, it is effectively a measure of the operational mode of a neuron as well and it determines where the neuron's activity lies on the continuum between pure temporal integration and pure coincidence detection.

Spike train distance metrics are a family of methods for calculating the dissimilarity (distance) between spike trains [21, 20, 11, 8, 22, 9, 10, 15]. Such measurements for spike trains are useful for quantifying the differences and similarities of spike timings across a number of trials with common stimuli [20], or measuring the spike time synchrony within a neural sub-population [11, 8, 9, 10]. In the case of the Victor-Purpura spike train distance metric, the dissimilarity between two spike trains is expressed as the cost of converting one spike train to another, in a similar fashion to the more general *edit-length distance* for sequences of characters or symbols [22]. More recently, Rusu & Florian [15] introduced the modulus-metric, a spike train metric inspired by the *Pompeiu-Hausdorff distance* [12, 4] between two nonempty, compact sets. The modulus metric computes the distances between two spike trains and the set of all possible spike trains within a bounded period [15]. The SPIKE-distance relies on instantaneous differences between nearby spikes from two spike trains and constructs a temporal profile of differences between the spike sequences [9].

When analysing multiple spike trains, the aforementioned metrics can be used to calculate the average pairwise distance, however this calculation scales with N^2 (where N is the number of spike trains), making such calculations infeasible for even a few dozen spike trains. A variant for multiple spike trains, the multivariate SPIKE-distance, can be calculated using the standard deviation of spike times following or preceding a point in time, which scales with N [9] and for this reason it was chosen for the work presented in the paper. The same study would be infeasible if average pairwise spike train distance metrics were used, or it would force us to limit the number of input spike trains (denoted in this work by N_{in} to specify that the spike trains are acting as inputs). Additionally, the SPIKE-distance is time-scale independent and parameter free, which reduces the complexity of our analysis further.

In the main part of this paper, we investigate the relation between the operational mode, as determined by the NPSS and the spike time distance of the spike trains driving the neuron, as measured by the SPIKE-distance metric. Our goal is to determine the circumstances under which input synchrony directly determines operational mode (i.e., high synchrony causes coincidence detection while low synchrony causes temporal integration) and more importantly, to investigate how the properties of the input (number of inputs, rate), combined with the properties of the neuron itself (synaptic weight, membrane leak time constant and threshold) affect this relationship.

Generally, the meaning of the two measures can be interpreted as *actual synchrony* for the SPIKE-distance versus *utilised synchrony* for the NPSS. In the former case, the SPIKE-distance is derived directly from the spike trains and is a measure of the synchrony between them, unaffected by spike rates or the properties of the neuron. On the other hand, the NPSS is a measure of how the neuron utilises the synchrony in the input; whether synchronous spike trains are solely responsible for causing response spikes, no coincidences are responsible for causing response spikes, or any combination in between.

In the rest of this paper, we initially describe the methodology and parameters used to generate synchronous spike trains and the model used to run the simulations. We then describe the calculation of the two measures, the SPIKE-distance and the NPSS, in detail. We continue with presenting our results and conclude with a detailed discussion of the relationship between the two measures and the various ways in which it is shaped by the values of the parameters used, both to generate the spike trains and to run the simulation.

2. Methods.

The overall methodology used is as follows:

1. Generate spike trains with parameter values (number of spike trains N_{in}, spike frequency f_{in}, fraction of synchronous spike trains S_{in} and jitter σ_{in}) randomised within the ranges defined in Table 1.
2. Calculate the multivariate SPIKE-distance (D_S) between the generated (input) spike trains (using the method described in [9], see also Section 2.2).
3. Use the spike trains to drive a neuron model, causing it to fire. The weight (depolarisation caused per spike, W_{in}) is also randomised and shown in Table 1.
4. Calculate the NPSS (using the method described in [7], see also Section 2.4).
5. Compare the NPSS with D_S.

In step 3, if the parameter value combination is such that no spikes are fired, the simulation is discarded entirely.

2.1. Input generation.

For step 1, we use the same method for generating synchronous spike trains as in [7]:

1a. Generate a single Poisson spike train with rate f_{in}.
1b. Copy the first spike train ($S_{in}N_{in} - 1$) times, resulting in $S_{in}N_{in}$ identical spike trains.
1c. Apply jitter to the generated spike trains by shifting each spike by a random variate from a Gaussian distribution with location 0 and standard deviation σ_{in}.
1d. Generate $N_{in}(1 - S_{in})$ Poisson spike trains, for a total of N_{in} spike trains.

TABLE 1. Parameter symbols and value ranges

Symbol	Description	Value or range	Units
N_{in}	Number of input spike trains	30–400	—
S_{in}	Fraction of trains that are synchronous	0–1	—
f_{in}	Input spike frequency per train	50–150	Hz
W_{in}	Input weight (voltage change per spike)	0.1–1.0	mV
σ_{in}	Gaussian jitter (for synchronous spikes)	0–4	ms
V_{th}	Neuron spike threshold	15	mV
V_0	Neuron resting (and reset) potential	0	mV
τ	Membrane leak time constant	10	ms

2.2. **SPIKE-distance.** The multivariate SPIKE-distance metric (step 2) is calculated using the method described in [9] and section 2.1.3 of that paper in particular. For any time t, the spike distance is:

$$S^m(t) = \frac{\sigma\left[t_P^{(n)}(t)\right]_n \langle X_F^{(n)}(t)\rangle_n + \sigma\left[t_F^{(n)}(t)\right]_n \langle X_P^{(n)}(t)\rangle_n}{\langle X_{ISI}^{(n)}(t)\rangle_n^2}, \tag{1}$$

Where $\langle X_P^{(n)}(t)\rangle_n$ and $\langle X_F^{(n)}(t)\rangle_n$ are the average intervals to the previous and following spikes respectively, across all N_{in} spike trains and $\sigma\left[t_P^{(n)}(t)\right]_n$ and $\sigma\left[t_F^{(n)}(t)\right]_n$ are their standard deviations. Finally, $\langle X_{ISI}^{(n)}(t)\rangle_n$ is the average ISI across the N_{in} spike trains, around time t.

To represent the SPIKE-distance value of the full duration of a simulation, we calculate the integral of S^m across time:

$$D_S = \frac{1}{T}\int_{t=0}^{T} S^m(t)dt \tag{2}$$

Numerically, the SPIKE-distance was computed at intervals for t of 1 ms and the integral was calculated using the trapezoidal rule.

2.3. **Neuron model.** In step 3, we use the leaky integrate-and-fire (LIF) model, as in [7], with total reset.

$$\tau\frac{dV}{dt} = V_0 - V(t) + RI(t) \tag{3}$$

The parameters for the resting potential V_0, spike threshold V_{th} and membrane leak time constant τ were the same as in [7] and are shown in Table 1. The rest of the parameters include R, which is the resistance of the membrane and $I(t)$, which is the time-dependent input current generated by incoming spikes. In our modelling, the input term $RI(t)$ is parameterised using W_{in} (in volts), which defines the voltage change per spike. Input spikes are treated as pulses, causing instantaneous changes in the membrane potential.

2.4. **Normalised Pre-Spike Slope.** In step 4, we calculate the NPSS after running the LIF neuron with the generated inputs from step 1 for 5 seconds of simulated time. The NPSS is calculated as follows:

4a. Calculate the mean slope of the membrane potential (m) in a time window ($w = 2$ ms) prior to the time of firing of each spike (t_i).

$$m_i = \left(V(t_i) - V(t_i - w)\right)/w \tag{4}$$

The value of w, also referred to as the *coincidence window*, is determined in part by the membrane leak time constant (τ) and the assumed temporal precision of the neuron [7].

4b. Calculate the upper (U) and lower (L_i) normalisation bounds for each inter-spike interval (ISI). Note that the upper bound does not depend on the length of the ISI (Δt_i), so it takes the same value in all cases:

$$U = (V_{th} - V_0)/w \tag{5}$$

$$L_i = \left[V_{th} - \left(V_0 + I_a\left(1 - e^{-\frac{\Delta t_i - w}{\tau}}\right)\right)\right]/w \tag{6}$$

$$I_a = (V_{th} - V_0)\,/\left(1 - e^{-\frac{\Delta t_i}{\tau}}\right). \tag{7}$$

The lower bound depends on I_a, which is the constant input that is required to cause the neuron to fire at exactly Δt_i, the length of the ISI.

4c. The NPSS value for the spike fired at t_i is given by:

$$M_i = (m_i - L_i)\,/\,(U - L_i)\,. \tag{8}$$

To represent the NPSS value of the full duration of a simulation, we use the arithmetic mean:

$$\bar{M} = \sum_i M_i \tag{9}$$

2.5. **Comparison.** Comparisons between the NPSS and the SPIKE-distance metric are made on averages across each simulation, i.e., $\overline{M}$ and D_S (eqns. 2 and 9).

3. **Results and discussion.** Our results initially focus on the relationship between the NPSS and the SPIKE-distance for all simulations. We look at the effect of several parameters and properties of the simulation on the relationship between the two measures and discuss its causes and implications. We then generalise our conclusions regarding the effect of synchrony on the operational mode.

The SPIKE-distance (D_S) is an inverse measure of synchrony. $D_S = 0$ indicates that all spike trains are synchronous (identical) while larger numbers indicate less synchrony. In our simulations, the maximum value of D_S approached 0.5, which is in accordance with the values shown in [9]. The NPSS ($\overline{M}$) indicates the operational mode by measuring the degree of utilised synchrony and ranges from 0 to 1. $\overline{M} = 0$ indicates that there is no synchrony responsible for the firing of the neuron, while $\overline{M} = 1$ means that the neuron fires solely due to synchronous spike trains.

For the following analysis, we introduce two features of the model: the asymptotic threshold-free potential (V_∞) and the volley peak potential (Δ_v). The asymptotic threshold-free potential is the asymptotic temporal mean of the membrane potential in the absence of a spike threshold and is calculated as follows:

$$V_\infty = N_{in} f_{in} W_{in} \tau. \tag{10}$$

The volley peak potential is the increase in potential at the membrane of the neuron when a completely synchronous volley arrives from all input spike trains and is calculated as follows:

$$\Delta_v = N_{in} W_{in}. \tag{11}$$

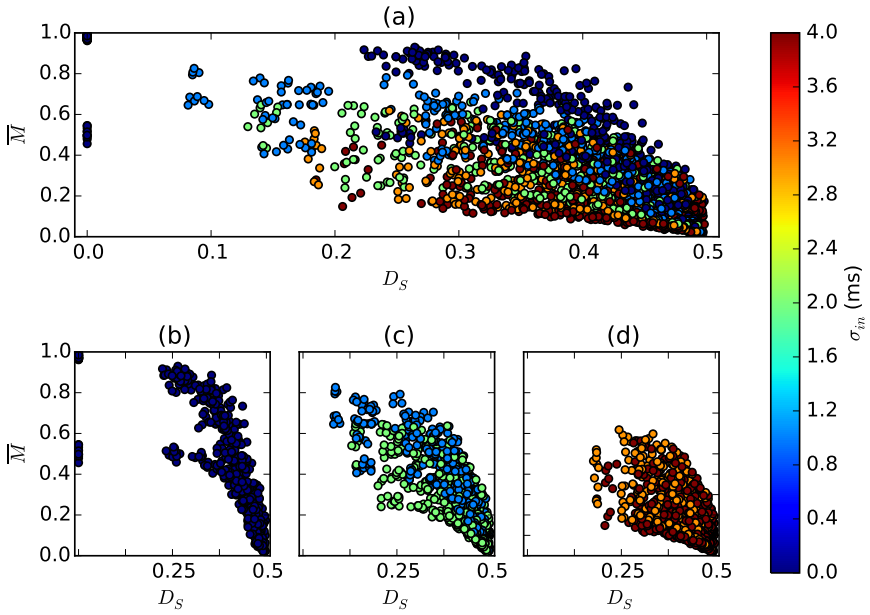

FIGURE 1. NPSS ($\overline{M}$) vs SPIKE-distance (D_S) with the colour of each point showing the degree of applied jitter (σ_{in}). High values mean high degrees of applied jitter (up to 4 ms) which makes spike volleys wider, while low values indicate that volleys are tighter and more synchronous, with 0 ms indicating that all spikes in a volley are simultaneous. (a) shows all points while the three smaller figures split the point into subsets depending on the value of σ_{in}. (b) $\sigma_{in} = 0$ ms. (c) 0 ms $< \sigma_{in} \leq 2$ ms. (d) $\sigma_{in} \geq 2$ ms.

3.1. **Effect of jitter (σ_{in}).** Fig. 1a shows the relationship between the multivariate SPIKE-distance and the NPSS for each simulation. The data consists of 605 simulations where no jitter was added to synchronous spike trains ($\sigma_{in} = 0$ ms) and 2420 simulations with jitter falling within the value ranges shown in Table 1 (3025 total). Figs. 1b to 1d show the same data, split into three cases, depending on the degree of jitter. For Fig. 1b, $\sigma_{in} = 0$ ms, for Fig. 1c, 0 ms $< \sigma_{in} \leq 2$ ms and for Fig. 1d, 2 ms $\leq \sigma_{in}$ (up to 4 ms). The maximum value for σ_{in} of 4 ms was chosen such that it is high enough to reduce synchrony significantly, to the point where no synchronous activity beyond what is expected by random chance remains, even for cases where $S_{in} = 1$ [7]. In all three figures, the colour of each point represents the value of jitter applied, denoted by the colour bar on the right-hand side.

In [7], we noted that increasing jitter from 0 to 4 ms, causes the operational mode to shift from coincidence detection to temporal integration. This is especially apparent in cases where volleys are supra-threshold ($\Delta_v > V_{th}$, see below) and presynaptic firing is completely synchronised ($S_{in} = 1$). In such cases, the value of σ_{in} can cause the neuron to operate as a pure coincidence detector (if $\sigma_{in} = 0$ ms, $\overline{M} = 1$) or a pure temporal integrator (if $\sigma_{in} \geq 4$ ms, $\overline{M} = 0$). The data presented in Fig. 1 generalises this conclusion, since as the jitter increases, the data points tend to stay closer to the lower-right of the plot, where the SPIKE-distance is

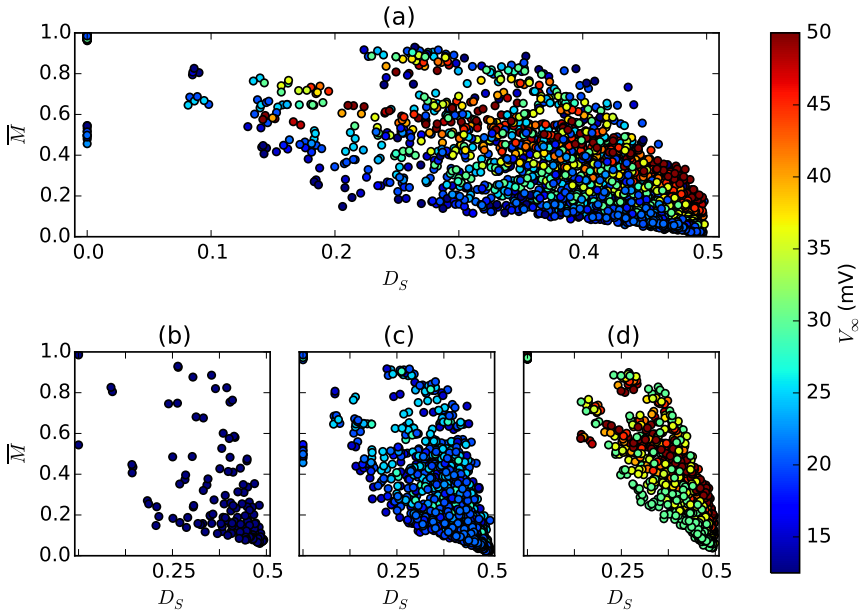

FIGURE 2. NPSS ($\overline{M}$) vs SPIKE-distance (D_S) with the colour of each point showing the asymptotic threshold-free potential (V_∞, see eqn. 10). (a) shows all points while the three smaller figures split the point into subsets depending on the value of V_∞ with respect to the spike threshold (V_{th}). (b) $V_\infty < V_{th}$. (c) $V_{th} \leq V_\infty < 2V_{th}$. (d) $V_\infty \geq 2V_{th}$.

high ($D_S > 0.25$) and the NPSS is low ($\overline{M} < 0.5$). This is expected, since lower synchrony, caused by higher jitter, causes the neuron to operate as a temporal integrator, regardless of any other behaviour or parameter.

3.2. **Effect of threshold-free potential (V_∞) and volley peak potential (Δ_v).** Fig. 2 shows the same data as Fig. 1, with the colour of each point representing the asymptotic, threshold-free potential (V_∞, eqn. 10). If V_∞ is higher than the spike threshold V_{th}, response spikes are generated almost surely, while if it is sub-threshold, response spikes are generated only if there is enough noise causing fluctuations that could drive the potential above threshold. The three smaller subfigures, Figs. 2b to 2d, separate the points into three categories, based on the relationship between V_∞ and V_{th}. For Fig. 2b, $V_\infty < V_{th}$, for Fig. 2c, $V_{th} \leq V_\infty < 2V_{th}$ and for Fig. 2d, $V_\infty \geq 2V_{th}$.

Similarly, Fig. 3 shows the same data again, but with the colour of each point representing the peak voltage change caused by a synchronous volley (Δ_v, eqn. 11). The three smaller subfigures, Figs. 3b to 3d, separate the points into three categories, based on the relationship between Δ_v and V_{th}. For Fig. 3b, $\Delta_v < V_{th}$, for Fig. 3c, $V_{th} \leq \Delta_v < 2V_{th}$ and for Fig. 3d, $\Delta_v \geq 2V_{th}$.

These two features define various aspects of the behaviour of the neuron as well as the relationship between the two measures being studied here (the SPIKE-distance and the NPSS). In particular, in the following sections, we will use the relationship

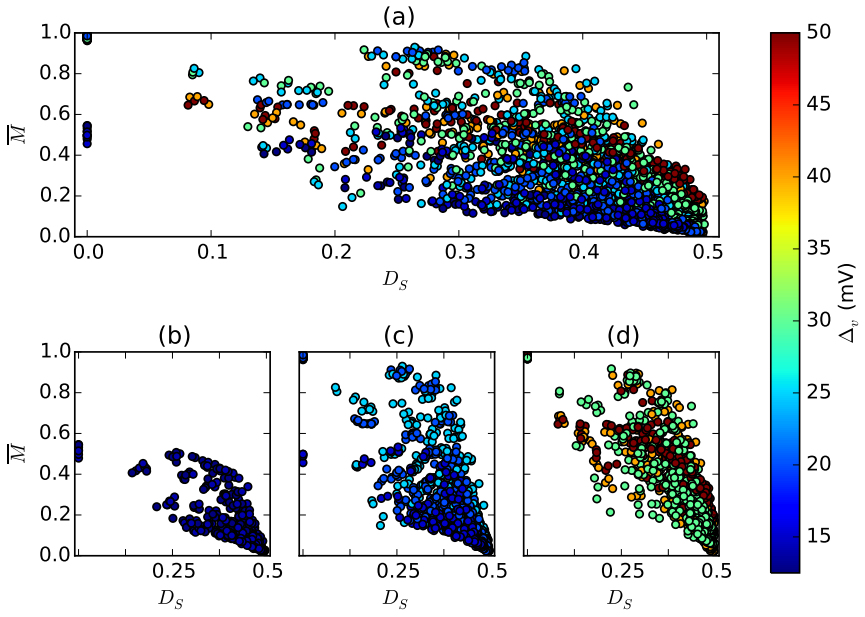

FIGURE 3. NPSS ($\overline{M}$) vs SPIKE-distance (D_S) with the colour of each point showing the peak depolarisation of a fully synchronous volley (Δ_v, see eqn. 11). (a) shows all points while the three smaller figures split the point into subsets depending on the value of Δ_v with respect to the spike threshold (V_{th}). (b) $\Delta_v < V_{th}$. (c) $V_{th} \leq \Delta_v < 2V_{th}$. (d) $\Delta_v \geq 2V_{th}$.

between these two values and the spike threshold (i.e., whether they are supra- or sub-threshold) to show how the relationship between the input synchrony and operational mode changes under different conditions.

3.3. **Integration of coincident volleys.** The data points in Fig. 1b that do not follow the trend seen in the other points of the same subfigure (points where $\overline{M} \approx 0.5$ and $D_s < 0.3$) are of particular interest. This deviation is caused by sub-threshold values for the asymptotic potential (V_∞) and more importantly the volley peak (Δ_v). This is evident in Figs. 2b, 2c, 3b and 3c which show the behaviour occurring for low values of V_∞ and Δ_v. Even more clearly, the phenomenon is exemplified in Figs. 4c, 5e and 5f, which show how the operational mode is determined by varying degrees of input synchrony when the asymptotic potential (V_∞) is above threshold and the volley peak (Δ_v) is below threshold. The phenomenon can also be seen in Figs. 4a, 5a and 5b, which show cases where both V_∞ and Δ_v are below threshold. More specifically, when $\Delta_v < V_{th}$, coincidence detection cannot occur, even for $S_{in} = 1$, since a single spike volley cannot bring the neuron to fire from rest. Instead, the neuron may *integrate* multiple spike volleys in order to reach the firing threshold and in that case, the NPSS measures a balance of integration and coincidence detection ($\overline{M} \approx 0.5$). The points that appear at $\overline{M} \approx 0.5$ and $D_S = 0$ on the figures are examples of this occurrence: the input spike trains were completely synchronous ($S_{in} = 1$) and there was no jitter ($\sigma_{in} = 0$ ms), which

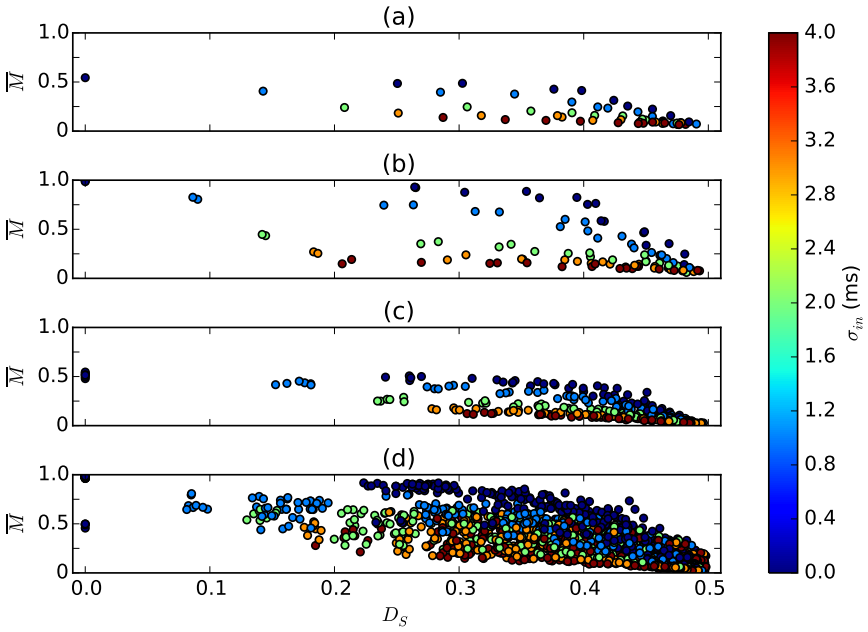

FIGURE 4. NPSS ($\overline{M}$) vs SPIKE-distance (D_S) with the colour of each point showing the degree of applied jitter (σ_{in}). Each subplot is separated based on the relationship of the asymptotic threshold-free potential (V_∞) and the volley peak (Δ_v) to the spike threshold (V_{th}). (a) Sub-threshold asymptotic potential and sub-threshold peak: $V_\infty < V_{th}$ & $\Delta_v < V_{th}$. (b) Sub-threshold asymptotic potential and supra-threshold peak: $V_\infty < V_{th}$ & $\Delta_v \geq V_{th}$. (c) Supra-threshold asymptotic potential and sub-threshold peak: $V_\infty \geq V_{th}$ & $\Delta_v < V_{th}$. (d) Supra-threshold asymptotic potential and supra-threshold peak: $V_\infty \geq V_{th}$ & $\Delta_v \geq V_{th}$.

results in a SPIKE-distance of zero, but the neuron behaves in a manner signified by the middle of the operational mode continuum, where neither pure coincidence detection nor temporal integration is taking place. In this case, we describe the behaviour of the neuron as *integrating coincidences*, to denote that high degrees of synchrony are driving the neuron, but multiple volleys are required to fire. In terms of the aforementioned *actual* versus *utilised* synchrony, the input spike trains have very high degrees of actual synchrony, but the neuron utilises this synchrony in a different way. Instead, the high synchrony in a single volley is only utilised to bring the membrane potential up to a certain level below threshold, before subsequent volleys are integrated to raise the membrane potential above threshold and trigger a response.

3.4. **Coincidence detection.** Our results also show the necessary circumstances for a neuron to operate as a coincidence detector. Coincidence detection is measured by the NPSS when $\overline{M} \approx 1$. We know that coincidence detection only occurs for high values of S_{in} and in fact, pure coincidence detection only occurs when $S_{in} = 1$. This is fundamental to our interpretation of the continuum of operational modes.

For any value $S_{in} < 1$, there are $N_{in}(1 - S_{in})$ random spike trains that contribute to the depolarisation of the membrane across each inter-spike interval. Therefore, a response spike cannot be fired as a result of coincident inputs only; there is always a degree of depolarisation that occurred before the coincidence window w and is part of the interval's integration period. By looking at each figure, we can determine how each of the other parameters and variables (σ_{in}, V_∞, Δ_v) affect the possibility of achieving pure coincidence detection. From Fig. 1 it is apparent that coincidence detection only occurs when $\sigma_{in} = 0$ ms (see, Fig. 1b), while Fig. 2 shows that the asymptotic potential, V_∞, has no effect on the ability of a neuron to operate as a coincidence detector. Finally, Fig. 3 shows that coincidence detection requires supra-threshold volley peaks, $\Delta_v \geq V_{th}$. The above is summarised in Fig. 4, which shows that coincidence detection occurs when $\Delta_v \geq V_{th}$ and $\sigma_{in} = 0$ ms (dark blue points in upper-left corner), but V_∞ can be either supra- or sub-threshold (Figs. 4b and 4c). Examples of pure coincidence detection occurring can also be seen in the sample configurations in Fig. 5. Figs. 5c and 5d show two cases where the asymptotic potential is sub-threshold and the volley peak is supra-threshold ($V_\infty = 10$ mV, $\Delta_v = 20$ mV for Fig. 5c and $V_\infty = 12.5$ mV, $\Delta_v = 25$ mV for Fig. 5d) and in both cases, $\overline{M} = 1$ when $S_{in} = 1, D_S = 0$ and $\sigma_{in} = 0$ ms. The same holds for Figs. 5g and 5h, which show two cases where the asymptotic potential and the volley peak are supra-threshold ($V_\infty = 25$ mV, $\Delta_v = 25$ mV for Fig. 5e and $V_\infty = 20$ mV, $\Delta_v = 40$ mV for Fig. 5f).

3.5. **Effect of input parameter values (N_{in}, f_{in}, W_{in}).** The figures for separate parameter configurations in Fig. 5 illustrate how the individual parameters of the neuron and the input have little effect on the relationship between the NPSS and the SPIKE-distance and it is in fact the volley peak's relation to the spike threshold that mostly defines the relationship. The relationship between the asymptotic potential and the threshold mainly determines the number of spikes that are fired when there is little or no synchrony. Cases where the asymptotic potential is sub-threshold and there is no synchrony simply produce very few spikes or none at all. Cases where no spikes were fired were discarded and therefore do not appear in any of the results. Each pair of figures in Fig. 5 shows very similar behaviour between them, suggesting that specific parameter values (N_{in}, f_{in}, W_{in}), or specific values for V_∞ & Δ_v are not important for the interaction between SPIKE-distance and NPSS, but the relative value of V_∞ towards the threshold is the most important factor.

3.6. **Summary of results.** In all figures, the horizontal axis represents the value of the integral of the SPIKE-distance over the entire duration of each simulation (D_S) and the vertical axis represents the value of the average NPSS ($\overline{M}$). The location of each point on a figure tells us the degree of synchrony in the input and how that synchrony is being utilised by the neuron. To summarise, we describe the causes and implications of points existing in each of the four quadrants of the plane defined by the two measures.

Points in the lower-right part of the plot denote cases where the input is mostly random (D_S is high) and the neuron is simply integrating random input spikes ($\overline{M}$ is low). This is the most common case, since it occurs both when S_{in} is low and when S_{in} and σ_{in} are both high.

Points in the upper-right part denote cases where the input is mostly random (D_S is high) but the neuron is performing coincidence detection. This case is rare and is caused by the SPIKE-distance measuring low spike train synchrony due to a

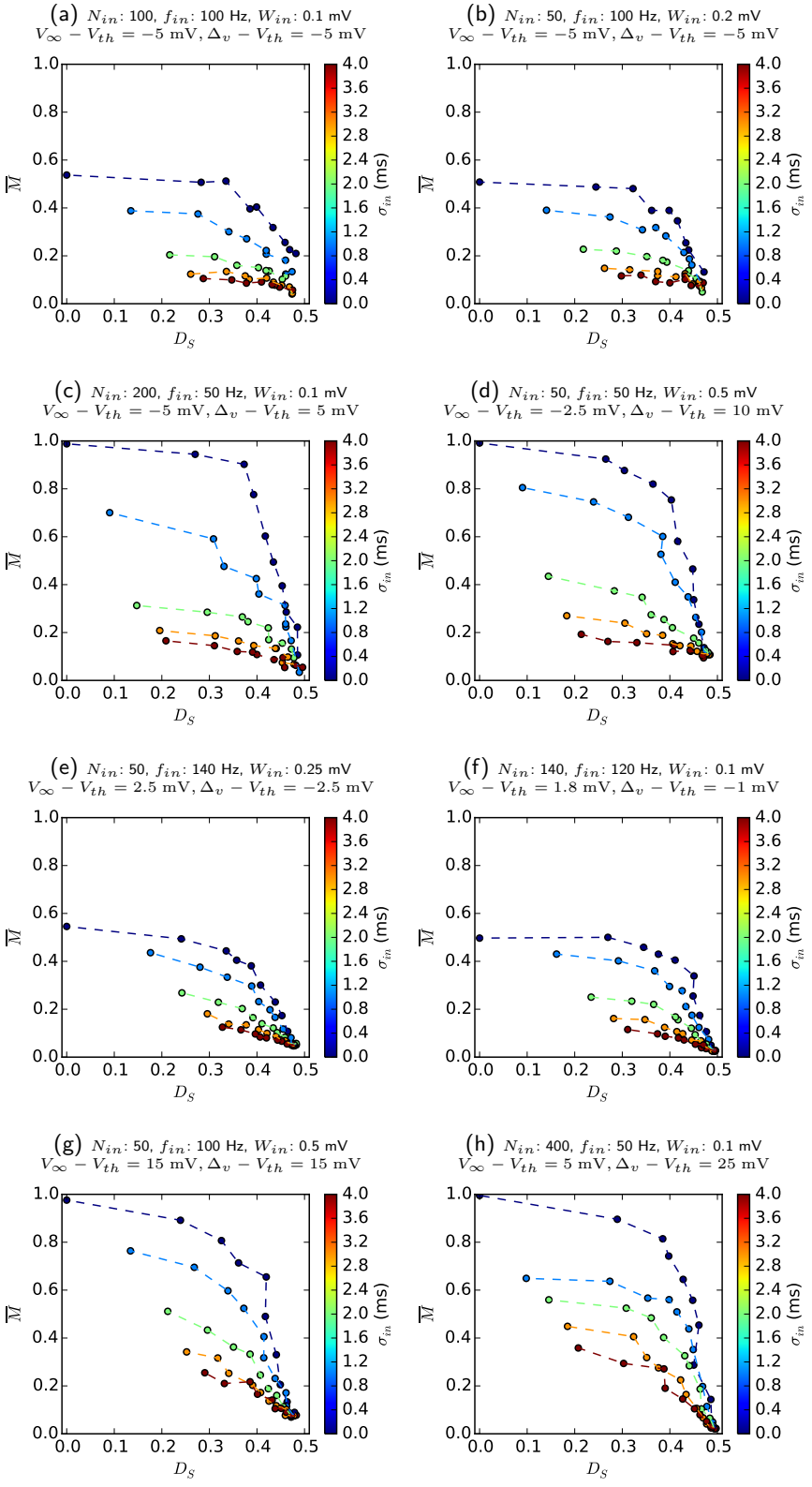
(a) N_{in}: 100, f_{in}: 100 Hz, W_{in}: 0.1 mV
$V_\infty - V_{th} = -5$ mV, $\Delta_v - V_{th} = -5$ mV
(b) N_{in}: 50, f_{in}: 100 Hz, W_{in}: 0.2 mV
$V_\infty - V_{th} = -5$ mV, $\Delta_v - V_{th} = -5$ mV
(c) N_{in}: 200, f_{in}: 50 Hz, W_{in}: 0.1 mV
$V_\infty - V_{th} = -5$ mV, $\Delta_v - V_{th} = 5$ mV
(d) N_{in}: 50, f_{in}: 50 Hz, W_{in}: 0.5 mV
$V_\infty - V_{th} = -2.5$ mV, $\Delta_v - V_{th} = 10$ mV
(e) N_{in}: 50, f_{in}: 140 Hz, W_{in}: 0.25 mV
$V_\infty - V_{th} = 2.5$ mV, $\Delta_v - V_{th} = -2.5$ mV
(f) N_{in}: 140, f_{in}: 120 Hz, W_{in}: 0.1 mV
$V_\infty - V_{th} = 1.8$ mV, $\Delta_v - V_{th} = -1$ mV
(g) N_{in}: 50, f_{in}: 100 Hz, W_{in}: 0.5 mV
$V_\infty - V_{th} = 15$ mV, $\Delta_v - V_{th} = 15$ mV
(h) N_{in}: 400, f_{in}: 50 Hz, W_{in}: 0.1 mV
$V_\infty - V_{th} = 5$ mV, $\Delta_v - V_{th} = 25$ mV
$\overline{M}$
D_S
σ_{in} (ms)

FIGURE 5. NPSS ($\overline{M}$) vs SPIKE-distance (D_S) for specific configurations of N_{in}, f_{in} and W_{in}, across the full range of synchrony parameters, $S_{in} \in [0, 1]$ (0.1 step size) and $\sigma_{in} \in [0, 4]$ ms (1 mV step size). The colour of each point shows the degree of applied jitter (σ_{in}). The dashed lines connect points which share the same value of σ_{in} and are ordered based on the value of S_{in}. Each subsequent point on a given line, starting from the top left, has a higher value of S_{in}. Therefore, each pair of figures correspond to one of the four cases shown in Fig. 4: (a) and (b) correspond to the first case (Fig. 4a) where both the asymptotic potential and the volley peak are sub-threshold, (c) and (d) correspond to the second case (Fig. 4b) where the asymptotic potential is sub-threshold and the volley peak is supra-threshold, (e) and (f) correspond to the third case (Fig. 4c) where the asymptotic potential is supra-threshold and the volley peak is sub-threshold, and (g) and (h) correspond to the fourth case (Fig. 4d) where both the asymptotic potential and the volley peak are supra-threshold.

large number of random spike trains, but the NPSS measures coincidence detection because the neuron is responding primarily to coincidences. A clear example of this occurrence can be seen in Fig. 5c, where $\overline{M} \approx 0.9$ and $D_S \approx 0.4$. Similar occurrences can also be seen in Figs. 5d, 5g and 5h. Even though $S_{in} = 0.8$ & $\sigma_{in} = 0$ ms (for Fig. 5c), which means that 80 % of spike trains are identical, the large value of $N_{in} = 200$ creates enough random spike trains for the SPIKE-distance to measure high overall spike distance. On the other hand, the NPSS measures a dominance of coincidence detection, due to the high synchrony driving the neuron.

Even less common are points in the lower-left part of the plots. This area denotes cases where the input is highly synchronous but the neuron performs mostly temporal integration (both D_S and $\overline{M}$ are low). Such cases can occur, theoretically, when the inputs are highly synchronised ($S_{in} \approx 1$ & $\sigma_{in} \approx 0$), the volley peak is very low ($\Delta_v \ll V_{th}$), but the input rate of each spike train (f_{in}) is very high, which causes a high asymptotic potential ($V_\infty > V_{th}$). The result of this, is an extreme case of the aforementioned behaviour of *integrating coincidences*, where the coincidences (synchronous volleys) cause very small depolarisation (low peak), but they are frequent enough to drive the membrane potential above threshold and cause response spikes. As far as the NPSS is concerned, this is equivalent to temporal integration, even though the spike trains at the input are highly synchronised. Our data does not show extreme versions of this case (e.g., points in the lower-left corner) since that would require very high spike rates. This can be seen by considering eqns. 10 and 11. Eqn. 10 can be rewritten as $V_\infty = \Delta_v f_{in} \tau$ and, since we consider τ constant for a given neuron, only the value of f_{in} can cause the asymptotic potential to become supra-threshold in the presence of a sub-threshold volley peak. For example, for $\Delta_v < 1$ mV (very small volley peak) the NPSS will measure near-zero, even when $S_{in} = 1$, but the asymptotic potential must be supra-threshold ($V_\infty \geq V_{th}$) for spikes to occur. Given our neuron parameter values, $V_{th} = 15$ mV and $\tau = 10$ ms, the individual input spike rate would have to be at least 1500 Hz.

The fourth and final case is represented by the upper-left part of the plot, where the input spike trains are highly synchronised (D_S is low) and the neuron is performing coincidence detection ($\overline{M}$ is high). As mentioned in Section 3.4, high input

synchrony, which occurs when S_{in} is high and σ_{in} is low, causes the neuron to operate as a coincidence detector only when the volley peak is supra-threshold ($\Delta_v > V_{th}$).

4. **Conclusions.** Through our study of the relationship between the NPSS and the SPIKE-distance metric, we have investigated the ways in which input synchrony determines the operational mode and how this relationship is affected by the properties of the pre-synaptic spike trains and the post-synaptic cell. The operational mode of a neuron is considered to exist in a continuum between temporal integration and coincidence detection [14, 7]. Generally, highly correlated or synchronised inputs are more likely to cause a post-synaptic response (spike reliability is increased) and shrink the response latency, two main characteristics of coincidence detection [2, 5, 14, 7, 13]. Therefore, it is generally believed that higher degrees of input synchrony cause the neuron to operate as a coincidence detector and conversely, random, or highly dispersed inputs cause the neuron to operate as a temporal integrator.

Our results and analysis show that high synchrony brings a neuron's operational mode to pure coincidence detection only when (i) the synchronous volley causes a high enough depolarisation to cause a response ($\Delta_v \geq V_{th}$) and (ii) spike volleys are highly synchronous ($\sigma_{in} = 0$ ms). These conditions are both necessary and sufficient for a neuron to operate in a pure coincidence detection mode, as measured by the NPSS. More generally, we have found that the relationship between input synchrony and operational mode is not straightforward. The most important factor is the amount of depolarisation caused by a single synchronous volley, assuming no jitter is applied (Δ_v). The relationship between this value and the post-synaptic neuron's spike threshold (V_{th}) greatly affects the relationship between input synchrony and operational mode. As already mentioned, when Δ_v is supra-threshold, higher degrees of input synchrony bring the neuron closer to coincidence detection. However, at lower values, the neuron begins to operate in a manner we have described as *integrating coincidences*, where a neuron is driven by high synchrony, but requires multiple highly synchronous volleys to reach the threshold.

Our measure could be adapted to measure the operational mode of more complex models which implement more realistic mechanisms. Such mechanisms may cause the neuron to prefer one operational mode over another intrinsically. For instance, active conductances can make the model more sensitive to synchronous inputs, which would favour coincidence detection and increase the frequency of high membrane potential slope values. The ability of the NPSS to correctly measure the response-relevant input synchrony depends mainly on whether the upper and lower slope bounds can reflect the effects of the neural mechanisms. This could be accomplished by determining the maximum and minimum rate of depolarisation empirically, by driving the model with inputs representing various extreme cases. It is unclear how this will affect the relationship between the NPSS and the SPIKE-distance, however. Certain neural mechanisms can cause the model to behave differently, even when driven by the same input spike patterns, under different conditions (e.g., for different degrees of membrane depolarisation). Whether a meaningful relationship between the two measures exists in such cases could be a matter of study that would follow the adaptation of the NPSS to different models and circumstances, and is outside the scope of this paper.

Acknowledgments. The authors gratefully acknowledge the support of the University of Cyprus for a scholarship under the programme "Young Researchers" (Νέοι Ερευνητές). They also would like to acknowledge the projects EGI – European Grid Infrastructure and "eMammoth – Compute and Store on Grids and Clouds infrastructure" (ANABATHMISI/06609/09), which is co-funded by the Republic of Cyprus and the European Regional Development Fund of the EU. The authors are also grateful to the two anonymous referees for their constructive and stimulating comments.

REFERENCES

[1] M. Abeles, Role of the cortical neuron: integrator or coincidence detector?, *Israel Journal of Medical Sciences*, **18** (1982), 83–92.

[2] A. Aertsen, M. Diesmann and M.-O. Gewaltig, Propagation of synchronous spiking activity in feedforward neural networks, *Journal of Physiology Paris*, **90** (1996), 243–247.

[3] G. Bugmann, C. Christodoulou and J. G. Taylor, Role of temporal integration and fluctuation detection in the highly irregular firing of a leaky integrator neuron model with partial reset, *Neural Computation*, **9** (1997), 985–1000.

[4] F. Hausdorff, *Grundzüge der Mengenlehre*, Verlag von Veit & Comp., Leipzig, 1914.

[5] M. A. Kisley and G. L. Gerstein, The continuum of operating modes for a passive model neuron, *Neural Computation*, **11** (1999), 1139–1154.

[6] P. König, A. K. Engel and W. Singer, Integrator or coincidence detector? The role of the cortical neuron revisited, *Trends in Neurosciences*, **19** (1996), 130–137.

[7] A. Koutsou, C. Christodoulou, G. Bugmann and J. Kanev, Distinguishing the causes of firing with the membrane potential slope, *Neural Computation*, **24** (2012), 2318–2345.

[8] T. Kreuz, D. Chicharro, R. G. Andrzejak, J. S. Haas and H. D. I. Abarbanel, Measuring multiple spike train synchrony, *Journal of Neuroscience Methods*, **183** (2009), 287–299.

[9] T. Kreuz, D. Chicharro, M. Greschner and R. G. Andrzejak, Time-resolved and time-scale adaptive measures of spike train synchrony, *Journal of Neuroscience Methods*, **195** (2011), 92–106.

[10] T. Kreuz, D. Chicharro, C. Houghton, R. G. Andrzejak and F. Mormann, Monitoring spike train synchrony, *Journal of Neurophysiology*, **109** (2013), 1457–1472.

[11] T. Kreuz, J. S. Haas, A. Morelli, H. D. I. Abarbanel and A. Politi, Measuring spike train synchrony, *Journal of Neuroscience Methods*, **165** (2007), 151–161.

[12] D. Pompeiu, Sur la continuité des fonctions de variables complexes, *Annales de la Faculté des Sciences de Toulouse*, **7** (1905), 265–315.

[13] S. Ratté, M. Lankarany, Y.-A. Rho, A. Patterson and S. A. Prescott, Subthreshold membrane currents confer distinct tuning properties that enable neurons to encode the integral or derivative of their input, *Frontiers in Cellular Neuroscience*, **8** (2014), 452.

[14] M. Rudolph and A. Destexhe, Tuning neocortical pyramidal neurons between integrators and coincidence detectors, *Journal of Computational Neuroscience*, **14** (2003), 239–251.

[15] C. V. Rusu and R. V. Florian, A new class of metrics for spike trains, *Neural Computation*, **26** (2014), 306–348.

[16] M. N. Shadlen and W. T. Newsome, Noise, neural codes and cortical organization, *Current Opinion in Neurobiology*, **4** (1994), 569–579.

[17] M. N. Shadlen and W. T. Newsome, The variable discharge of cortical neurons: Implications for connectivity, computation, and information coding, *Journal of Neuroscience*, **18** (1998), 3870–3896.

[18] W. R. Softky and C. Koch, Cortical cells should fire regularly, but do not, *Neural Computation*, **4** (1992), 643–646.

[19] W. R. Softky and C. Koch, The highly irregular firing of cortical cells is inconsistent with temporal integration of random EPSPs, *Journal of Neuroscience*, **13** (1993), 334–350.

[20] J. D. Victor, Spike train metrics, *Current Opinion in Neurobiology*, **15** (2005), 585–592.

[21] J. D. Victor and K. P. Purpura, Metric-space analysis of spike trains: Theory, algorithms and application, *Network: Computation in Neural Systems*, **8** (1997), 127–164.

[22] J. D. Victor and K. P. Purpura, Spike metrics, in *Analysis of Parallel Spike Trains* (eds. S. Grün and S. Rotter), Springer Series in Computational Neuroscience, 7, Springer US, Boston, MA, 2010, 129–156.

Received March 24, 2015; Accepted November 02, 2015.

E-mail address: achilleas.k@cs.ucy.ac.cy
E-mail address: jkanev@zoho.com
E-mail address: mariaeconomidou@hotmail.com
E-mail address: cchrist@cs.ucy.ac.cy